

The Kynurenine Pathway and Inflammation in Amyotrophic Lateral Sclerosis

Yiquan Chen · Roger Stankovic · Karen M. Cullen · Vincent Meininger · Brett Garner · Sarah Coggan · Ross Grant · Bruce J. Brew · Gilles J. Guillemin

Received: 20 May 2009 / Revised: 22 September 2009 / Accepted: 27 October 2009
© Springer Science+Business Media, LLC 2009

Abstract Amyotrophic lateral sclerosis (ALS) is a progressive and fatal motor neuron disease of unknown pathogenesis. The kynurenine pathway (KP), activated during neuroinflammation, is emerging as a possible contributory factor in ALS. The KP is the major route for tryptophan (TRP) catabolism. The intermediates generated can be either neurotoxic, such as quinolinic acid (QUIN), or neuroprotective, such as picolinic acid (PIC), an important endogenous chelator. The first and inducible

enzyme of the pathway is indoleamine 2,3-dioxygenase (IDO). The present study aimed to characterize the expression of the KP in cerebrospinal fluid (CSF), serum and central nervous system (CNS) tissue of ALS patients. Using high performance liquid chromatography, we analysed the levels of TRP and kynurenine (KYN), and, with gas chromatography/mass spectrometry, the levels of PIC and QUIN, in the CSF and serum of ALS patients and control subjects. Immunohistochemistry was employed to determine the expression of QUIN, IDO and human leukocyte antigen-DR (HLA-DR) in sections of brain and spinal cord from ALS patients. There were significantly increased levels of CSF and serum TRP ($P < 0.0001$), KYN ($P < 0.0001$) and QUIN ($P < 0.05$) and decreased levels of serum PIC ($P < 0.05$) in ALS samples. There was a significant increase in activated microglia expressing HLA-DR ($P < 0.0001$) and increased neuronal and microglial expression of IDO and QUIN in ALS motor cortex and spinal cord. We show the presence of neuroinflammation in ALS and provide the first strong evidence for the involvement of the KP in ALS. These data point to an inflammation-driven excitotoxic-chelation defective mechanism in ALS, which may be amenable to inhibitors of the KP.

Y. Chen · S. Coggan · R. Grant · G. J. Guillemin (✉)
Department of Pharmacology, School of Medical Sciences,
University of New South Wales, Sydney, NSW 2052, Australia
e-mail: G.Guillemin@unsw.edu.au;
g.guillemin@cfi.unsw.edu.au

B. J. Brew · G. J. Guillemin
St. Vincent's Centre for Applied Medical Research,
Darlinghurst 2010, Australia

B. J. Brew
Department of Neurology, St. Vincent's Hospital,
Darlinghurst 2010, Australia

R. Stankovic · K. M. Cullen
Anatomy and Histology, School of Medical Sciences,
The University of Sydney, Sydney, NSW 2006, Australia

V. Meininger
Centre for SLA, Hôpital Pitié-Salpêtrière, APHP, Paris, France

R. Grant
Australasian Research Institute, Sydney Adventist Hospital,
Sydney, NSW 2076, Australia

B. Garner
Prince of Wales Medical Research Institute, Randwick,
NSW 2031, Australia

Keywords Amyotrophic lateral sclerosis · Kynurenine pathway · Excitotoxicity · Neuroinflammation

Introduction

Amyotrophic lateral sclerosis (ALS) is the most common form of adult motor neuron disease, typically afflicting those around 50–60 years of age. Betz cells in the motor cortex and motor neurons in the brainstem and ventral horn

of the spinal cord are selectively targeted, resulting in loss of motor units, general muscle weakness and atrophy, paralysis and, ultimately, death (Bruijn et al. 2004). The progression is rapid, and death usually occurs within 5 years of disease onset (Bruijn et al. 2004). Approximately 90% of ALS cases are sporadic and only 10% are familial, of which 20% can be attributed to mutations in the copper/zinc superoxide dismutase (SOD1) gene (Rosen et al. 1993). The current drug treatment options are meagre. The only drug approved for ALS treatment by the Food and Drug Administration in the USA, riluzole, targets a single putative cause (glutamate cytotoxicity) of the disease and extends a patient's life by an average of only 2 months (Bensimon et al. 1994; Lacomblez et al. 1996). There are, however, other mechanisms hypothesized to be associated with the neuropathology of ALS, including oxidative stress, microfilament abnormality, dysfunction of the microtubular transport system, abnormal protein aggregation and glial cell pathology (Rothstein 2009). Investigation of the kynurenine pathway (KP), and quinolinic acid (QUIN) in particular, has potential to provide direct evidence to link these hypotheses.

Although multiple mechanisms are likely to contribute to ALS, disease progression may be driven by the common process of inflammation. The “first hit” of this process may inflict a non-lethal injury to motor neurons of individuals with a susceptible genetic constitution, in turn triggering a progressive inflammatory process (“second hit”) that activates microglia, the resident immune cells of the brain, which produce neurotoxic compounds that further destroy motor neurons. Indeed, activated microglia are key intrinsic participants in neuroinflammation and a common feature around injured and degenerating neurons (Streit 2002).

In the CNS, initiation of the immune response involves the release of inflammatory mediators, such as tumour necrosis factor alpha (TNF- α), interleukin-6 (IL-6), IL-1 β , interferon gamma (IFN- γ), prostaglandin E2 and activation of the enzyme cyclooxygenase (Shaw 2005). In addition, the KP, the major route for tryptophan (TRP) catabolism, is activated during neuroinflammation in several neurodegenerative diseases, such as Alzheimer's disease (Guillemin et al. 2005b), and may play a role in ALS (Guillemin et al. 2005a). The KP yields nicotinamide adenosine dinucleotide and generates both neuroprotective and neurotoxic intermediates. The first stable intermediate in the pathway is kynurenine (KYN). Subsequent intermediates include the neuroprotectants, kynurenic acid (KYNA), an *N*-methyl-D-aspartic (NMDA) receptor antagonist (Perkins and Stone 1982) and picolinic acid (PIC) (Kalisch et al. 1994), a potent endogenous chelator, and the excitotoxin and NMDA receptor agonist, QUIN (Stone and Perkins 1981). The first enzyme initiating the KP is either tryptophan 2,3-dioxygenase (TDO) or indoleamine 2,3-

dioxygenase (IDO) (Salter and Pogson 1985; Takikawa et al. 1986). Within the CNS, IDO is the predominant enzyme, expressed by most human brain cells (Guillemin et al. 2000; Guillemin et al. 2001, 2005b, 2007; Owe-Young et al. 2008), and is activated by immune-related molecules, such as lipopolysaccharides and inflammatory cytokines, particularly IFN- γ (Yoshida and Hayaishi 1978).

In the present study of ALS patients, we analysed cerebrospinal fluid (CSF) and serum samples for levels of TRP, KYN, PIC and QUIN and post-mortem brain and spinal cord for HLA-DR, IDO and QUIN in an attempt to determine the role of the KP in the inflammatory response and progression of ALS.

Methods and Materials

CSF and Serum Samples from ALS and Control Patients

The present study was approved by the Human Ethics Committees of the University of New South Wales (H03-037), the University of Sydney (HREC 09-2008/11256), Hôpital Pitié-Salpêtrière and the Sydney Adventist Hospital (SAH HREC 13/2). We studied 140 matching CSF and serum samples from ALS and control patients. ALS samples were provided by Prof. Meininger from the ALS Centre at the Hôpital Pitié-Salpêtrière in Paris, France. All ALS patients fulfilled the El Escorial criteria for definite or probable ALS (Brooks et al. 2000) and were all undergoing treatment with riluzole at the time of CSF and serum collection. Of the ALS samples ($n = 140$), 47% were female, with an average disease onset age of 58.3 ± 12.3 years, and 53% were male, with an average disease onset of 58.2 ± 12.0 years. Patients included both sporadic and familial ALS, with either bulbar or limb onset. The control samples ($n = 35$), average age of 35.8 ± 3.0 years, were chosen from patients at the Sydney Adventist Hospital in NSW, Australia, who had undergone lumbar puncture for suspected meningitis but had normal cell count, protein and glucose levels in pathology tests and an absence of any disease during follow-up examinations. Control subjects had not taken any antimicrobial, steroidal or cytotoxic medication within 12 h of the procedure. Due to the limited amount of control CSF samples, 18 samples were exhausted during the gas chromatography–mass spectrometry (GC/MS) analysis, leaving 17 control samples for HPLC analysis.

High Performance Liquid Chromatography

The High Performance Liquid Chromatography (HPLC) method used here is a modification of a published protocol (Schrocksadel et al. 2006). CSF and serum samples were

analysed using an Agilent 1200 HPLC with Agilent ChemStation software (Santa Clara, CA, USA). 30 μ l samples were injected and analysed at a flow rate of 1 ml/min of ammonium acetate buffer (0.1 M, pH 4.65), using a C18 column, at 22°C. TRP was monitored by a fluorescence detector at an excitation wavelength of 285 nm, an emission wavelength of 365 nm, with a retention time of 17.5 min. KYN was monitored using a UV detector, set at 360 nm wavelength, with a retention time of 8.7 min. The index for IDO activity was determined by calculating the ratio of KYN/TRP concentrations.

Gas Chromatography–Mass Spectrometry

[2-²H₇]Picoline and [3-²H₇]Picoline were obtained from Cambridge Isotope Laboratories Inc. (Andover, MA, USA), and [²H₃]QUIN (99%) was from Le Research Inc. (St. Paul, MN, USA). PIC, QUIN, trifluoroacetic anhydride and 1,1,1,3,3,3-hexafluoro-2-propanol were obtained from Sigma-Aldrich (St. Louis, MO, USA), and reagent-grade organic solvents were obtained from commercial suppliers.

The GC/MS method used for the analysis of PIC and QUIN levels in CSF and serum has been previously described (Smythe et al. 2002). For the analysis, 1 μ l of sample was injected into an Agilent 6890 gas chromatograph, interfaced to an Agilent 5973 mass selective detector via an auto-sampler Agilent Technologies 7683, and controlled using Agilent ChemStation software (Agilent, Santa Clara, CA, USA).

Immunohistochemistry

Tissue sections of post-mortem motor cortex and cervical spinal cord were provided by the Tissue Resource Centre, the University of Sydney. Brain and spinal cord tissue was taken at autopsy, formalin fixed, blocked, embedded in paraffin and sectioned at 7 μ m. Tissue sections from 4 patients with sporadic ALS, 1 patient with progressive muscular atrophy (PMA) as a negative control for upper motor neuron lesions and 1 neurologically normal control were analysed. Post-mortem delay (PMD) was less than 10 h, except for case ALS4 (PMD of 20 h). ALS patients were aged 62.0 \pm 4.7 years, PMA aged 83 years and control aged 25 years. For the neurologically normal control, brain and spinal cord were taken at time of autopsy and were unremarkable macroscopically and microscopically as reported by a qualified neuropathologist. The post-mortem diagnosis of ALS was based on ubiquitin immunopositive (pAb 1:200, DakoCytomation, Glostrup, Denmark), skein-like inclusions in ventral horn motor neurons, a decreased number of Betz cells in cresyl violet stained sections of motor cortex, and degeneration of the lateral pyramidal tracts in Luxol fast blue stained sections of the spinal cord.

Immunohistochemistry

Several 7- μ m sections were taken from paraffin-embedded blocks of motor cortex and spinal cord, deparaffinised and rehydrated. Sections were taken through methanol-hydrogen peroxide solution and 0.1 M TRIS buffered saline (pH 7.6) and then labelled for QUIN mAb (1:50, developed by Millipore), HLA-DR mAb (1:100, DAKO) and, IDO mAb (1:200, Chemicon). Pre-treatment for antigen retrieval were as follows: for HLA-DR—heat induction 120°C, 20 min in citric acid buffer pH 6.0, for IDO and QUIN—proteinase K 10 μ g/ml in 5 mM TRIS, pH 8.0, and 0.5 mM EDTA for 8 min at 37°C.

HLA-DR positive microglia in ALS and control tissue were quantified by image analysis from digital micrographs, captured with a Jentopix Progres C14 digital camera attached to a Leica DMLB bright field microscope (Leica Microsystems Australia). For the spinal cord, 10 fields were randomly sampled from 4 sections of the lateral corticospinal tracts and the ventral horns. The histogram function in Adobe Photoshop (version CS2, Adobe systems, CA, USA) was used to determine the areal fraction of HLA-DR staining (e.g. percentage of the section occupied by HLA-DR labelling) in each field. The mean areal fraction from 10 sampled fields per case per region is reported.

In order to provide an overall view of microglia activation in the spinal cord, a photomontage of a HLA-DR labelled spinal cord section was compiled for case ALS-3. Using a 20 \times objective, 300 sequential and slightly overlapping photos of entire spinal cord were taken by stepping the stage at regular intervals in the *x* then *y* directions. The images were then merged into a single montage using the ‘automate/photomerge’ menu in Adobe Photoshop. Here, we present the data for only the right corticospinal tract and ventral horn as microglial densities in left and right spinal were not statistically different in any ALS case (see Results).

The degree of IDO and QUIN positive labelling in the ALS and control spinal cord sections were determined semi-quantitatively, through manual counting by an investigator blinded to the experiment, using the following rating: – (no staining), + (<50 cells); ++ (51–99 cells); +++ (>100 cells). Two spinal cord sections were sampled for each case and the values were averaged for the final scoring.

Statistical Analysis

For the HPLC and GC/MS data, Student’s *t*-test, ANOVA and regression with age analyses were done to assess the different factors—metabolite concentrations, age, gender and disease type (familial versus sporadic and limb onset versus bulbar onset). For the areal fraction immunohistochemical data,

Mann–Whitney test and regression with age analysis were performed. $P < 0.05$ was taken to be statistically significant in all instances.

Results

ALS Patients

There was no significant difference between gender and age of disease onset for either sporadic or familial ALS patients. Nor was there a difference between age of onset and disease type (familial versus sporadic). However, the age for bulbar onset ALS was significantly higher compared to limb onset ALS ($P < 0.01$), and there was 2.5 times more males than females with familial ALS.

High Performance Liquid Chromatography

For ALS patients, serum TRP levels were significantly higher ($P < 0.05$) in males (149.1 ± 17.0) compared to females ($118.9 \pm 8.4 \mu\text{M}$). Serum IDO activity was significantly lower ($P < 0.001$) in familial ALS (0.022 ± 0.003) compared to either CSF IDO activity (0.043 ± 0.01) or IDO activity in sporadic ALS (0.040 ± 0.003) (Table 1). Regression with age data analysis indicated no correlation between CSF or serum IDO activity, TRP or KYN levels with age in either ALS or control subjects. Compared to controls, ALS patients had significantly elevated levels of CSF and serum TRP and KYN ($P < 0.0001$) and CSF IDO activity ($P < 0.0001$). Comparing ALS patients to controls, the mean CSF TRP level was 5.0 ± 0.2 versus 2.6 ± 0.2

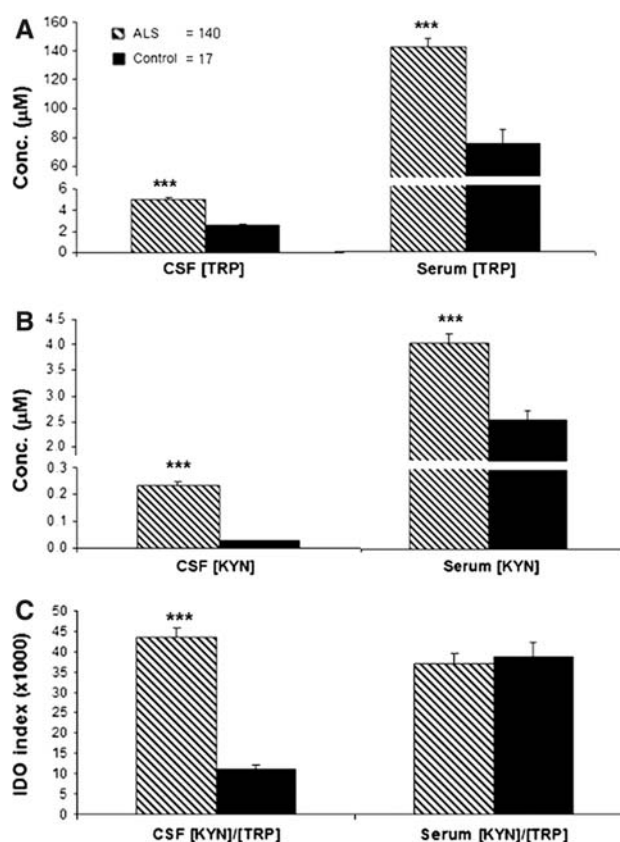


Fig. 1 TRP, KYN and IDO activity in CSF and serum samples of ALS and controls determined by HPLC. ALS patients ($n = 140$) had significantly higher levels of CSF TRP (a) and KYN (b) than controls ($n = 17$) ($P < 0.0001$). Serum levels of TRP and KYN were significantly higher in ALS patients than controls ($P < 0.0001$). c CSF IDO activity was significantly elevated in ALS patients ($P < 0.0001$) compared to controls

Table 1 QUIN, PIC, TRP, KYN concentration and IDO activity in ALS groups

	Controls ($n = 35^a/17$)	Male ($n = 74$)	Female ($n = 66$)	Sporadic ALS ($n = 133$)	Familial ALS ($n = 7$)	Limb onset ($n = 109$)	Bulbar onset ($n = 31$)
QUIN ^a , serum (μM)	0.30 ± 0.03	0.39 ± 0.02	0.35 ± 0.02	0.38 ± 0.02	0.36 ± 0.04	0.36 ± 0.02	0.43 ± 0.04
QUIN ^a , CSF (μM)	0.04 ± 0.00	0.05 ± 0.01	0.06 ± 0.01	0.05 ± 0.01	0.04 ± 0.01	0.05 ± 0.01	0.04 ± 0.01
PIC ^a , serum (μM)	2.4 ± 0.4	1.46 ± 0.13	1.47 ± 0.11	1.45 ± 0.09	1.80 ± 0.51	1.49 ± 0.10	1.45 ± 0.16
PIC ^a , CSF (μM)	0.51 ± 0.11	0.36 ± 0.04	0.37 ± 0.06	0.35 ± 0.07	0.60 ± 0.21	0.35 ± 0.07	0.30 ± 0.06
TRP, serum (μM)	75.0 ± 10.5	$149.1 \pm 17.0^*$	118.9 ± 8.4	133.3 ± 6.0	166.4 ± 20.7	137.3 ± 6.9	128.2 ± 10.6
TRP, CSF (μM)	2.58 ± 0.16	5.03 ± 0.58	4.23 ± 0.54	4.67 ± 0.19	5.20 ± 0.87	4.73 ± 0.22	4.58 ± 0.33
KYN, serum (μM)	2.52 ± 0.19	4.03 ± 0.46	3.96 ± 0.38	4.05 ± 0.21	3.24 ± 0.36	4.00 ± 0.24	3.99 ± 0.29
KYN, CSF (μM)	0.03 ± 0.00	0.22 ± 0.03	0.22 ± 0.03	0.22 ± 0.01	0.26 ± 0.05	0.22 ± 0.02	0.21 ± 0.03
IDO activity, serum	0.04 ± 0.00	0.04 ± 0.00	0.04 ± 0.00	0.04 ± 0.00	$0.02 \pm 0.00^{**}$	0.04 ± 0.00	0.04 ± 0.00
IDO activity, CSF	0.01 ± 0.00	0.04 ± 0.01	0.04 ± 0.01	0.04 ± 0.00	0.04 ± 0.01	0.04 ± 0.00	0.04 ± 0.00

There was no significant difference between serum and CSF in the concentration of KYN, QUIN and PIC in ALS groups or between genders. Serum TRP levels were significantly higher in males compared to females ($P < 0.05$). IDO activity in the serum was significantly lower in familial ALS compared to either CSF IDO activity in familial ALS or IDO activity in sporadic ALS ($P < 0.01$)

^a $n = 35$

* $P < 0.05$; ** $P < 0.001$

μM , CSF KYN level was 0.23 ± 0.02 versus 0.027 ± 0.000 μM , serum TRP level was 143.3 ± 5.6 versus 75.0 ± 10.5 μM , serum KYN level was 4.0 ± 0.2 versus 2.5 ± 0.2 μM (Fig. 1a, b), CSF IDO activity was 0.044 ± 0.002 versus 0.011 ± 0.001 and serum IDO activity was 0.037 ± 0.0025 versus 0.039 ± 0.004 (Fig. 1c).

Gas Chromatography–Mass Spectrometry

There was no significant difference between age-matched female and male population within either the ALS or control group ($P > 0.05$) for QUIN and PIC concentrations. Regression with age data analysis indicated no correlation between CSF or serum QUIN or PIC levels with age in either ALS or control subjects. Serum PIC levels were significantly lower ($P < 0.05$) in ALS compared to controls, while CSF PIC levels trended towards lower concentrations in ALS ($P = 0.09$). ALS patients had mean PIC serum and CSF concentrations of 1.4 ± 0.1 and 0.36 ± 0.03 μM , respectively, compared to 2.4 ± 0.4 and 0.51 ± 0.11 μM in controls. In contrast, CSF and serum QUIN levels were significantly higher ($P < 0.05$) in ALS patients, with mean concentrations of 0.053 ± 0.005 and

0.37 ± 0.02 μM , respectively, compared to 0.038 ± 0.004 and 0.30 ± 0.03 μM in controls (Fig 2).

Descriptive and Quantitative Immunohistochemistry

The ALS spinal cord montage (Fig. 3) showed an extensive inflammatory response, as indicated by numerous activated microglia (HLA-DR⁺) when compared to the control spinal cord that showed very few activated microglia with fainter cytoplasmic HLA-DR immunoreactivity. In ALS spinal cord, activated microglia were aggregated around regions of the spinal cord that are most affected in ALS pathology, namely the lateral corticospinal tract and ventral horn (Fig 4d). This distribution pattern of activated microglia was observed in all ALS cases in the present study.

There was neither a correlation between any measure and the age of patient nor a significant difference between the areal fraction of microglia in the left and right corticospinal tracts and ventral horns of the spinal cord ($P > 0.2$). ALS cases showed a highly significant increase in the percentage of activated microglia in the spinal cord compared to the control (Fig. 4c, d). In the corticospinal tract, the values ranged from 0.5 ± 0.07 to $1.3 \pm 0.05\%$ in ALS and

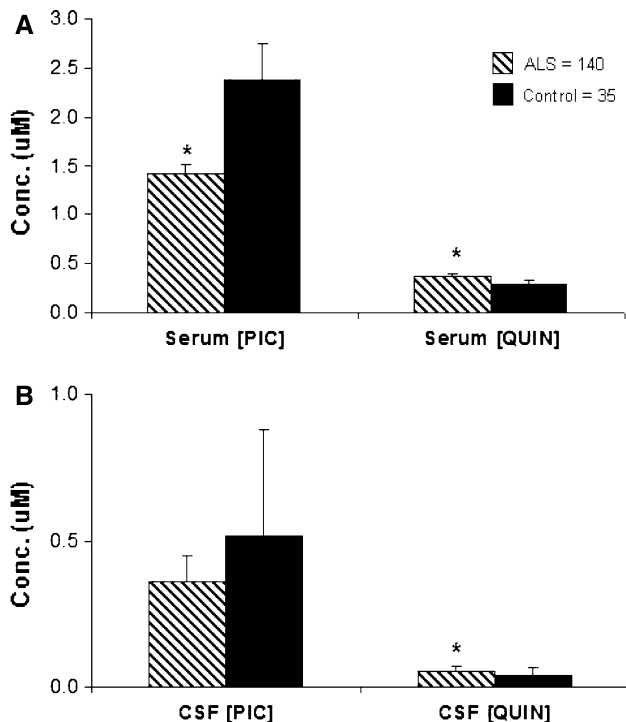


Fig. 2 CSF and serum levels of PIC and QUIN in ALS and controls determined by gas chromatography/mass spectrometry. **a** PIC serum levels were significantly lower ($P < 0.05$) in ALS patients ($n = 140$) compared to controls ($n = 35$), while **b** PIC CSF levels were higher in controls but this did not reach significance. **b** QUIN CSF and serum levels were significantly higher ($P < 0.05$) in ALS patients than controls

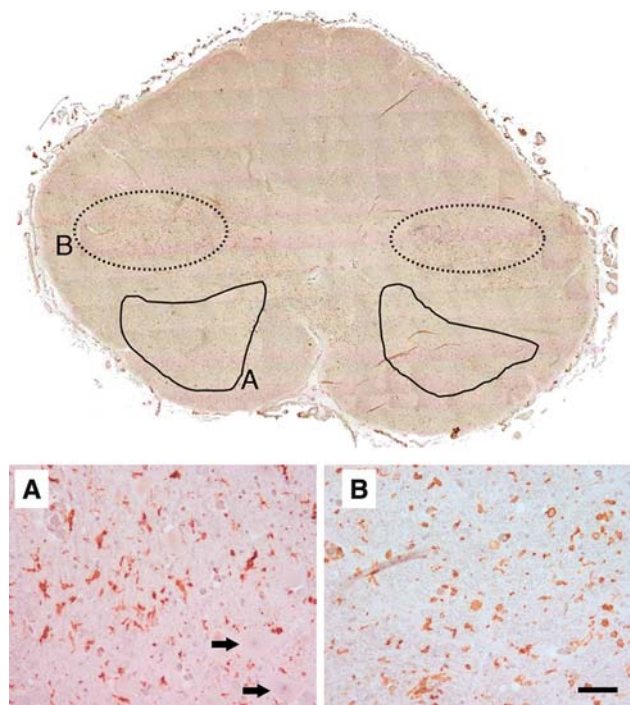


Fig. 3 HLA-DR expression in ALS spinal cord. Montages were assembled from photomicrographs taken with a $20\times$ objective by stepping the stage in the x - and y -axes. The *dashed traces* indicate approximate area of corticospinal and rubrospinal tracts and *solid outline* is of the ventral horns. High-magnification views from the montage are shown in (A) and (B). Significant numbers of reactive microglia (HLA-DR positive) are present in both areas. In the ventral microglia frequently surrounding palely stained residual motor neurons (*arrows*). Scale bar = $50 \mu\text{m}$ for (A) and (B)

0.01 ± 0.006 to 0.04 ± 0.006% in controls ($P < 0.001$) (Fig. 5a). Similarly, in the ventral horn, the areal fraction of activated microglia ranged from 0.3 ± 0.05 to 0.9 ± 0.02% in ALS and 0 to 0.02 ± 0.005% in controls ($P < 0.001$) (Fig. 5b). ALS sections also showed positive

ubiquitinated skein-like inclusions, which were used as part of disease diagnosis (Fig. 6e). Positive IDO (Fig. 6d) and QUIN (Fig. 7d) staining were also found in the cytoplasm of ventral horn motor neurons and in microglia from ALS spinal cord. Semi-quantitative analysis for IDO labelling

Fig. 4 HLA-DR expression in ALS and control motor cortex and spinal cord. Activated microglia (HLA-DR⁺) are seen in significant numbers in the motor cortex (a) of ALS case, in particular in layer V (arrows) of the M1 cortex where cortical pyramidal motor neurons (Betz cells) are located. Control motor cortex labelled for HLA-DR (b) showing low-level expression of HLA-DR in scattered resting microglia (inset). c Lateral pyramidal tract from control spinal cord showing little to no HLA-DR staining. d A view of the lateral pyramidal tract from ALS spinal cord showing HLA-DR expressing microglia encircling axon bundles. Scale bars = 400 μm for a and b; 50 μm for c and 100 μm for d

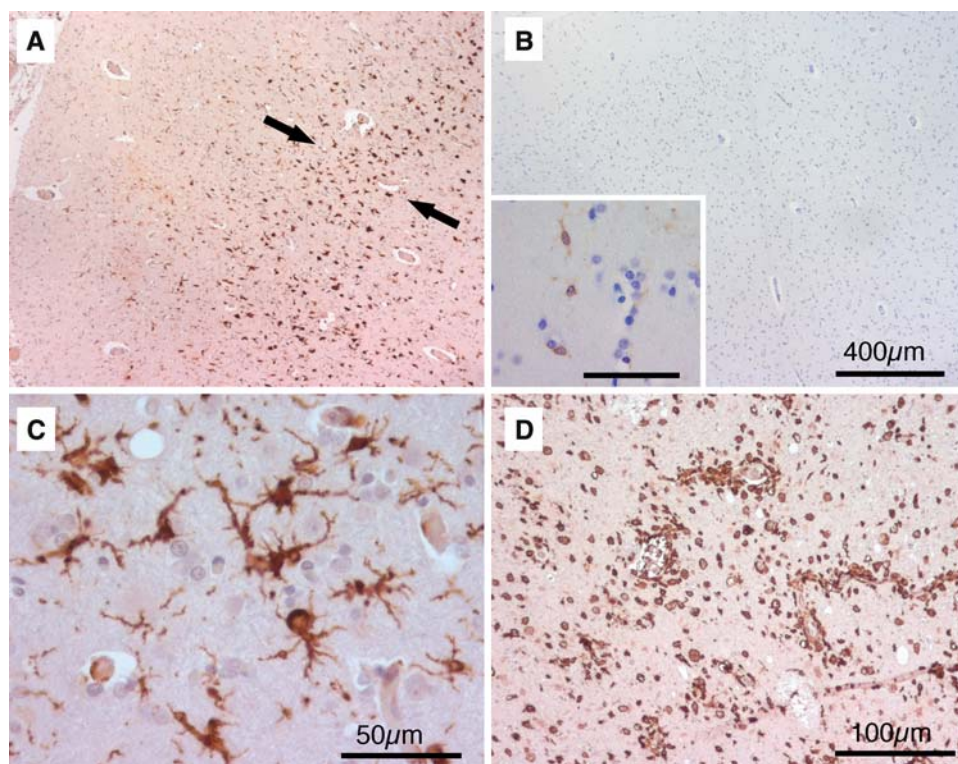


Fig. 5 Activated microglia in ALS and control spinal cord. a In the corticospinal tract, all 4 ALS cases had a significantly higher ($P < 0.0001$) areal fraction of activated microglia than either the PMA or control cases. The areal fraction ranged from 0.5 ± 0.07 to 1.3 ± 0.05% in ALS and 0.01 ± 0.006 to 0.04 ± 0.006% in controls. b In the ventral horn, a similar pattern was observed, whereby ALS cases had significantly more ($P < 0.0001$) activated microglia than either the PMA or control cases. The areal fraction ranged from 0.3 ± 0.05 to 0.9 ± 0.02% in ALS and 0 to 0.02 ± 0.005% in controls

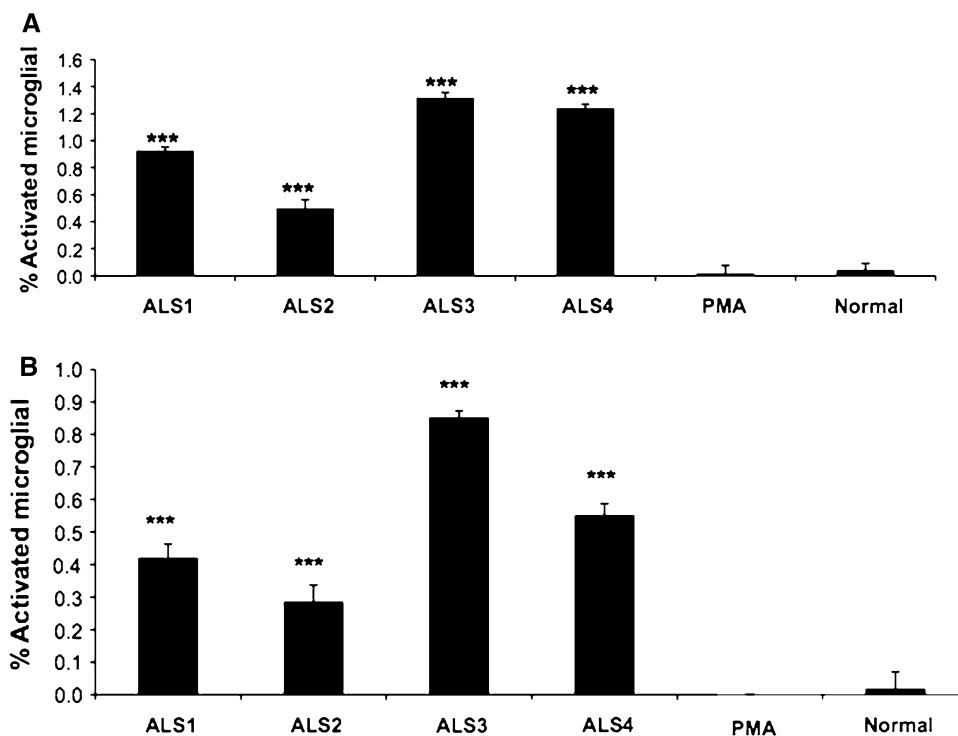
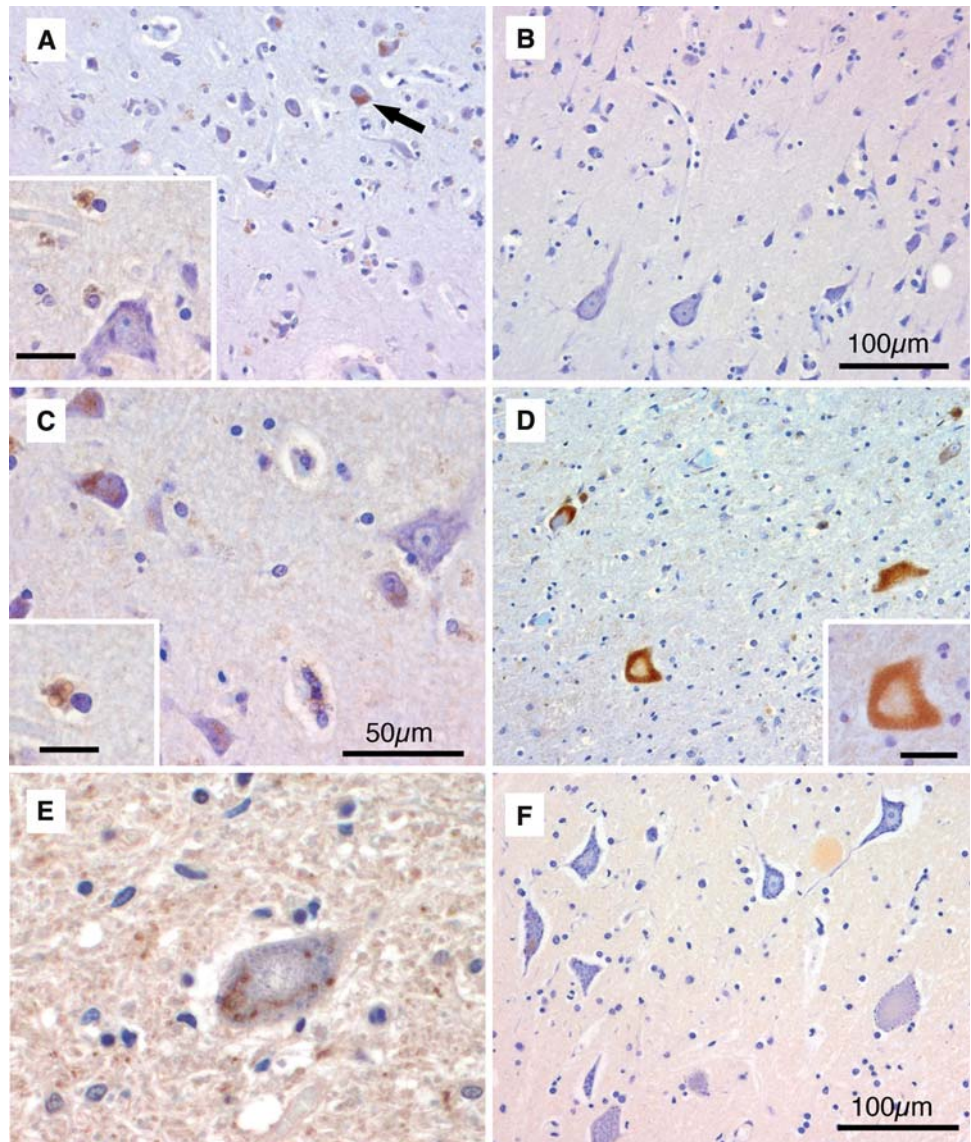


Fig. 6 IDO expression in ALS and control motor cortex and spinal cord. **a** Cytoplasmic expression of IDO in motor cortical neurons of in ALS brain (arrow indicates one positive neuron). *Inset* shows microglia expression of IDO nearby a Betz cell in the motor cortex. **b** Control motor cortex showing no positive labelling for IDO. **c** Motor cortex from a second ALS case showing cytoplasmic expression of IDO in neurons and vesicular-like labelling in an activated microglia (*inset*). **d** Ventral horn alpha motor neurons showing cytoplasmic IDO. *Scale bars* = 100 μ m for **a** and **b**; 100 μ m for **d** and **e**; 25 μ m for *insets*



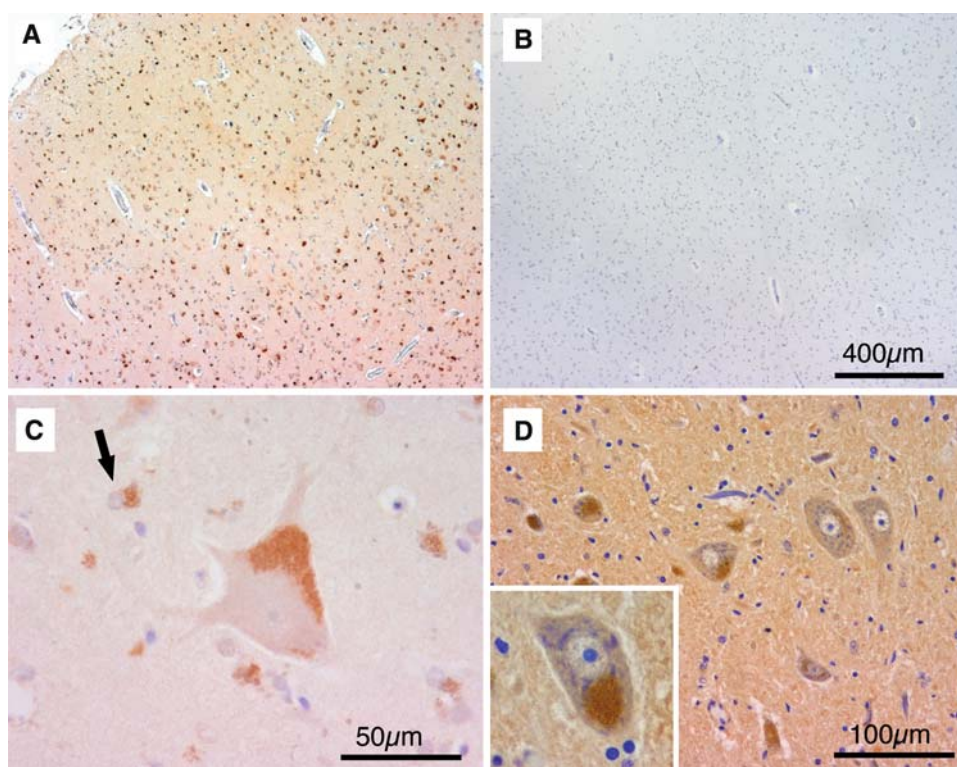
ranged between mild and moderate (+ to ++) in ALS, mild (+) in PMA and negative in controls (Fig. 6f). Degree of QUIN labelling was mild (+) in the control and high (+++) in ALS cases.

In ALS motor cortex, significant numbers of activated microglia were observed, occurring predominantly in layer V, where Betz cells are located, and in the M1 cortex (Fig. 4a). QUIN immunoreactivity was also seen mostly in motor neurons and microglia and cytoplasmic staining of QUIN in Betz cells was also evident (Fig. 7c). Likewise, IDO was found in the few remaining Betz cells and in microglia (Fig. 6a, c). In contrast, the control showed little or no positive staining for HLA-DR (Fig. 4b), IDO (Fig. 6b) or QUIN (Fig. 7b).

Discussion

The KP represents a major route in the catabolism of TRP and is implicated in several neurological disorders, including AIDS dementia complex (Guillemin et al. 2004), Parkinson's disease (Hartai et al. 2005) and Alzheimer's disease (Guillemin et al. 2005b). It has potent immunoregulatory properties, particularly in the prevention of T-cell mediated allogenic foetal rejection (Munn et al. 1998), suppression of cancer progression (Muller et al. 2005), T-cell proliferation and promotion of T-cell apoptosis (Frumento et al. 2002). Recent studies have bridged a direct association between the KP and ALS (Guillemin et al. 2005a). Ilzecka et al. (2003) demonstrated that ALS

Fig. 7 QUIN in ALS and control motor cortex and spinal cord. **a** Immunopositivity for QUIN in ALS, mainly in activated microglia, but also in pyramidal neurons and **b** little to no QUIN staining in control motor cortex. Although QUIN was detected in all layers of ALS cortex, positive cells were more concentrated in layer V of the M1 cortex. This pattern was less distinctly layered than for IDO. **c** Betz cells in ALS cases showed cytoplasmic QUIN immunopositivity, as do surrounding microglia (*arrow*). **d** Cytoplasmic expression of QUIN is also seen in ventral horn neurons (*inset*). Scale bars = 400 μ m for **a** and **b**; 50 μ m for **c** and *inset* in **d**; 100 μ m for **d**



patients with bulbar onset and severe clinical status had increased CSF KYNA levels. In contrast, serum KYNA levels were lower in patients with severe clinical status than in patients of mild clinical status or neurologically normal controls. In familial ALS cases, protein aggregation of mutant SOD-1 has been found to be mediated by TRP via oxidation and cross-linking of the enzyme (Bruijn et al. 1998; Watanabe et al. 2001; Zhang et al. 2003).

Our HPLC data show a twofold increase in CSF TRP, serum TRP and serum KYN, a tenfold increase in CSF KYN and a fourfold increase in intracellular CSF IDO activity in ALS compared to controls. Although KYN can be transported across the blood brain barrier, the tenfold increase in CSF KYN, compared to only a twofold increase in serum KYN, is strongly indicative of a CNS source. Due to the possible transport of TRP and KYN across the blood brain barrier, two separate IDO activities were determined—the periphery (from serum) and the CNS (from CSF). Although static measures of the TRP/KYN ratio are not a direct measure of enzyme activity, these measures provide a quantifiable estimate of changes in the KP metabolism. A distinction was not made between IDO and TDO activity in this case as the main objective was to determine whether the KP was stimulated. Since IDO is the predominant enzyme extrahepatically and TDO is only weakly expressed within the brain, KYN/TRP was taken to reflect IDO activity. The increased in IDO activity in patients was further supported in the immunohistochemistry data. It is important to note here that as all ALS patients

received riluzole treatment and there is currently no literature on the impact of riluzole on the KP, we cannot rule riluzole out as a potential contributing factor in the changes outlined above.

TRP is an essential amino acid and approximately 50–90% is protein-bound. However, this association is unstable and does not affect uptake of TRP into the CNS (Pardridge and Fierer 1990) via the non-specific L-system of the neutral amino acid transporter (Matsuo et al. 2000). There is enhanced IDO activity and accelerated TRP degradation in several neurodegenerative diseases (Widner et al. 2000, 2002). In contrast, our study reports an increase in TRP levels in ALS patients.

In healthy human subjects and rats, administration of a TRP load results in significant increase in oxidative stress in the brain, possibly through the generation of superoxide free radicals, hydrogen peroxide and hydroxyl radicals (Forrest et al. 2004, 2008). In familial ALS, the situation may be further aggravated by the promotion of SOD protein aggregates by TRP (Bruijn et al. 1998; Watanabe et al. 2001; Zhang et al. 2003). The elevated levels of serum and CSF TRP are speculated to reflect a dysfunction in protein binding and L-neutral amino acid transporters, respectively; or perhaps, an over-compensatory response, whereby the increase in CSF IDO activity results in a decrease in CSF TRP, which encourages the dissociation of TRP from albumin to facilitate transport of TRP across the blood brain barrier. In addition, riluzole, the main drug of choice for ALS treatment, is highly protein-bound. Thus, it

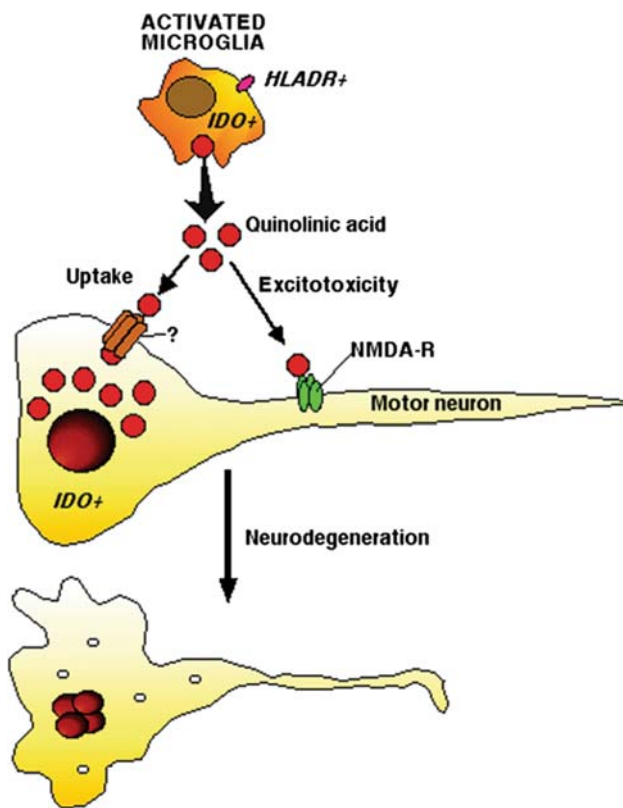


Fig. 8 A schematic diagram of QUIN toxicity in motor neurons. The presence of numerous activated microglia in ALS leads to the release of large amount of QUIN into the microenvironment. QUIN can then result in excitotoxicity in motor neurons via NMDA receptors or it can also be taken up in large quantities by motor neurons. Ultimately, excitotoxicity and the accumulation of QUIN contribute to the demise of motor neurons

is possible that riluzole displaces TRP from albumin leading to the observed increase in TRP. It is interesting to note that although both serum and CSF TRP and KYN were higher in ALS patients, increased IDO activity was seen only in the CNS.

Our GC/MS data show an increase in both CSF and serum QUIN levels and a decrease in serum PIC levels in ALS patients compared to controls. This suggests a disturbance in the KP in ALS, skewing towards neurotoxicity and away from neuroprotection. It is of significance as QUIN is a potent excitotoxin, whereas PIC is a neuroprotectant (Guillemin et al. 2007). In addition, any QUIN produced in the brain would be localised due to poor blood brain barrier permeability (Fukui et al. 1991). Hence, a weakening in neuroprotection may exacerbate the adverse effects of neurotoxicity. The immunohistochemistry of ALS brain and spinal cord further confirms the presence of cytoplasmic QUIN and IDO expression in microglia. Both QUIN and IDO are expressed in the few remaining Betz cells and ventral horn motor neurons. What is not yet understood is whether the QUIN produced in microglia is

externalised into the surrounding environment; and, if it is, whether motor neurons take up QUIN, perhaps via a still unidentified cell surface receptor (Fig. 8). A recently published study with glutamate found that abnormal neurons exhibit an up-regulation in a particular form of glutamate–aspartate transporter, which may make them more vulnerable to glutamate-mediated excitotoxicity (Sullivan et al. 2007). As such, a similar event is hypothesized to occur between QUIN and motor neurons.

Pathological concentrations of QUIN could result in a myriad of unfavourable consequences that could exacerbate and accelerate the condition of ALS. As an endogenous NMDA agonist, QUIN is a potent excitatory compound (Stone and Perkins 1981). In the brain, the main source of QUIN is immune cells rather than astrocytes or neurons (Guillemin et al. 2001, 2007). Indeed, astrocytes lack the enzyme kynurenine hydroxylase and are incapable of synthesizing QUIN (Guillemin et al. 2001). However, high levels of KYN produced by astrocytes can be taken up by surrounding activated microglia for QUIN production (Guillemin et al. 2001). Once QUIN exceeds the “safety threshold” (<150 nM), its adverse effect is exerted via the generation of reactive oxygen species (Santamaria et al. 2001), augmentation of the excitotoxic impact through disruption in the glutamatergic transport system, apoptosis, mitochondrial dysfunction and the production of cytokines and chemokines, all of which are putatively thought to be contributory factors in ALS (Fig. 8) (Guillemin et al. 2005a).

In contrast, PIC, a pyridine monocarboxylic acid, is an endogenous neuroprotectant in the brain and other tissues (Jhamandas et al. 1990). It displays neuroprotective properties against QUIN without affecting the excitatory aspect of QUIN (Cockhill et al. 1992; Beninger et al. 1994). The antagonism is also specific, as not all structurally similar compounds of PIC protect against QUIN (Cockhill et al. 1992). In addition, PIC can manipulate the immune response by stimulating chemokine production in macrophages (Bosco et al. 2000), and has anti-tumour (Leuthauser et al. 1982), antifungal (Blasi et al. 1993) and antiviral (Fernandez-Pol et al. 2001) properties. The mechanism of action of PIC is currently under investigation but is thought to involve intact glutamatergic afferent input and zinc chelation (Cockhill et al. 1992; Jhamandas et al. 1998). In ALS, the role of PIC as a zinc chelator may also be of importance as altered zinc binding and zinc transportation potentially contributes to the progression of ALS (Smith and Lee 2007). All mutant forms of SOD1 mice show changes in zinc binding capacity regardless of the location of the mutation, whether within or beyond the metal-binding region (Lyons et al. 1996). In addition, a reduction in the expression of the metallothionein zinc transporters in SOD1 mice leads to an earlier onset of symptoms and a shorter lifespan (Nagano et al. 2001).

As in many other neurodegenerative diseases, ALS is also characterized by neuroinflammation, observed in both familial and sporadic ALS and in the SOD1 transgenic mouse model of ALS (McGeer and McGeer 2002). In the present study, we show a significantly increased microglial activation in ALS motor cortex and spinal cord that is absent from both PMA and controls, indicating a heightened immune response in ALS CNS. The presence of other inflammation indicators, such as IgG, monocyte chemoattractant protein-1, T cells, macrophages, dendritic cells, and reactive astrocytes, have also been shown in ALS spinal cord (McGeer and McGeer 2002). A recent study also uncovered a novel interferon-signalling pathway between motor neurons and glial cells. In the region of degenerating motor neurons, several interferon stimulating genes were significantly up-regulated in glial cells in the pre-symptomatic stage of ALS in mice (Zhang 2007). When tested in vitro, the glial cells were highly sensitive to interferon in a time-and-dose dependent manner (Zhang 2007). IFN- γ is the most potent inducer of IDO and can activate and up-regulate the KP. In the brain, stimulation of microglia and perivascular macrophages by IFN- γ increases QUIN production (Heyes et al. 1996), which, in turn, up-regulates chemokine production and chemokine receptor expression in astrocytes, further propagating the inflammatory response (Guillemin et al. 2003).

In conclusion, our data support the involvement of the KP in ALS and, for the first time, show the elevation of TRP, IDO activity and neurotoxic QUIN in ALS, and the presence of QUIN and IDO in ALS brain and spinal cord. The increase in neurotoxin QUIN is of significance as it would result in increase excitotoxicity and oxidative stress, exacerbating motor neuron degeneration in ALS. As the glutamate modulator, riluzole, is the only drug currently approved for ALS treatment and studies support ALS as a multifactorial disease, combination therapies that target other pathogenic mechanisms may be more effective in slowing disease progression and prolonging survival (Brooks 2009). Compounds targeting the KP offer a novel and potentially effective treatment for ALS.

Acknowledgements This study was funded by the Motor Neuron Disease Research Institute Association (Australia). The NSW Tissue Resource Centre is supported by The University of Sydney, Schizophrenia Research Institute, National Institutes on Alcohol Abuse and Alcoholism (NIAAA-grant no: R01AAA01272508), Sydney South Western Area Health Service (SSWAHS).

References

- Beninger RJ, Colton AM, Ingles JL, Jhamandas K, Boegman RJ (1994) Picolinic acid blocks the neurotoxic but not the neuroexcitant properties of quinolinic acid in the rat brain: evidence from turning behaviour and tyrosine hydroxylase immunohistochemistry. *Neuroscience* 61:603–612
- Bensimon G, Lacomblez L, Meininger V, ALS/Riluzole Study Group (1994) A controlled trial of riluzole in amyotrophic lateral sclerosis. *N Engl J Med* 330:585–591
- Blasi E, Mazzolla R, Pitzurra L, Barluzzi R, Bistoni F (1993) Protective effect of picolinic acid on mice intracerebrally infected with lethal doses of *Candida albicans*. *Antimicrob Agents Chemother* 37:2422–2426
- Bosco MC, Rapisarda A, Massazza S, Melillo G, Young H, Varesio L (2000) The tryptophan catabolite picolinic acid selectively induces the chemokines macrophage inflammatory protein-1 alpha and -1 beta in macrophages. *J Immunol* 164:3283–3291
- Brooks BR (2009) Managing amyotrophic lateral sclerosis: slowing disease progression and improving patient quality of life. *Ann Neurol* 65:S17–S23
- Brooks BR, Miller RG, Swash M, Munsat TL (2000) El Escorial revisited: revised criteria for the diagnosis of amyotrophic lateral sclerosis. *Amyotroph Lateral Scler Other Motor Neuron Disord* 1:293–299
- Brujin LI, Houseweart MK, Kato S, Anderson KL, Anderson SD, Ohama E, Reaume AG, Scott RW, Cleveland DW (1998) Aggregation and motor neuron toxicity of an ALS-linked SOD1 mutant independent from wild-type SOD1. *Science* 281:1851–1854
- Brujin LI, Miller TM, Cleveland DW (2004) Unraveling the mechanisms involved in motor neuron degeneration in ALS. *Annu Rev Neurosci* 27:723–749
- Cockhill J, Jhamandas K, Boegman RJ, Beninger RJ (1992) Action of picolinic acid and structurally related pyridine carboxylic acids on quinolinic acid-induced cortical cholinergic damage. *Brain Res* 599:57–63
- Feksa LR, Latini A, Rech VC, Feksa PB, Koch GD, Amaral MF, Leipnitz G, Dutra-Filho CS, Wajner M, Wannmacher CM (2008) Tryptophan administration induces oxidative stress in brain cortex of rats. *Metab Brain Dis* 23:221–233
- Fernandez-Pol JA, Klos DJ, Hamilton PD (2001) Antiviral, cytotoxic and apoptotic activities of picolinic acid on human immunodeficiency virus-1 and human herpes simplex virus-2 infected cells. *Anticancer Res* 21:3773–3776
- Forrest CM, Mackay GM, Stoy N, Egerton M, Christofides J, Stone TW, Darlington LG (2004) Tryptophan loading induces oxidative stress. *Free Radic Res* 38:1167–1171
- Frumonto G, Rotondo R, Tonetti M, Damonte G, Benatti U, Ferrara GB (2002) Tryptophan-derived catabolites are responsible for inhibition of T and natural killer cell proliferation induced by indoleamine 2,3-dioxygenase. *J Exp Med* 196:459–468
- Fukui S, Schwarcz R, Rapoport SI, Takada Y, Smith QR (1991) Blood-brain barrier transport of kynurenines: implications for brain synthesis and metabolism. *J Neurochem* 56:2007–2017
- Guillemin GJ, Smith DG, Kerr SJ, Smythe G, Kapoor V, Armati PJ, Brew BJ (2000) Characterisation of kynurenine pathway metabolism in human astrocytes and implications in neuropathogenesis. *Redox Rep* 5:108–111
- Guillemin GJ, Kerr SJ, Smyth PG, Smith DG, Kapoor V, Armati PJ, Croitoru J, Brew BJ (2001) Kynurenine pathway metabolism in human astrocytes: a paradox for neuronal protection. *J Neurochem* 78:842–853
- Guillemin GJ, Croitoru-Lamoury J, Dormont D, Armati PJ, Brew BJ (2003) Quinolinic acid upregulates chemokine production and chemokine receptor expression in astrocytes. *Glia* 41:371–381
- Guillemin GJ, Kerr SJ, Brew BJ (2004) Involvement of quinolinic acid in AIDS dementia complex. *Neurotox Res* 7:103–124
- Guillemin GJ, Meininger V, Brew BJ (2005a) Implications for the kynurenine pathway and quinolinic acid in amyotrophic lateral sclerosis. *Neurodegener Dis* 2:166–176

- Guillemin GJ, Brew BJ, Noonan CE, Takikawa O, Cullen KM (2005b) Indoleamine 2,3 dioxygenase and quinolinic acid immunoreactivity in Alzheimer's disease hippocampus. *Neuropathol Appl Neurobiol* 31:395–404
- Guillemin GJ, Cullen KM, Lim CK, Smythe GA, Garner B, Kapoor V, Takikawa O, Brew BJ (2007) Characterization of the kynurenine pathway in human neurons. *J Neurosci* 27:12884–12892
- Hartai Z, Klivenyi P, Janaky T, Penke B, Dux L, Vecsei L (2005) Kynurenine metabolism in plasma and in red blood cells in Parkinson's disease. *J Neurol Sci* 239:31–35
- Heyes MP, Achim CL, Wiley CA, Major EO, Saito K, Markey SP (1996) Human microglia convert l-tryptophan into the neurotoxin quinolinic acid. *Biochem J* 320(Pt 2):595–597
- Ilzecka J, Kocki T, Stelmasiak Z, Turski WA (2003) Endogenous protectant kynurenine acid in amyotrophic lateral sclerosis. *Acta Neurol Scand* 107:412–418
- Jhamandas K, Boegman RJ, Beninger RJ, Bialik M (1990) Quinolinic acid-induced cortical cholinergic damage: modulation by tryptophan metabolites. *Brain Res* 529:185–191
- Jhamandas KH, Boegman RJ, Beninger RJ, Flesher S (1998) Role of zinc in blockade of excitotoxic action of quinolinic acid by picolinic acid. *Amino Acids* 14:257–261
- Kalisch BE, Jhamandas K, Boegman RJ, Beninger RJ (1994) Picolinic acid protects against quinolinic acid-induced depletion of NADPH diaphorase containing neurons in the rat striatum. *Brain Res* 668:1–8
- Lacomblez L, Bensimon G, Leigh PN, Guillet P, Meininger V, Amyotrophic Lateral Sclerosis/Riluzole Study Group II (1996) Dose-ranging study of riluzole in amyotrophic lateral sclerosis. *Lancet* 347:1425–1431
- Leuthauser SW, Oberley LW, Oberley TD (1982) Antitumor activity of picolinic acid in CBA/J mice. *J Natl Cancer Inst* 68:123–126
- Lyons TJ, Liu H, Goto JJ, Nersissian A, Roe JA, Graden JA, Cafe C, Ellerby LM, Bredesen DE, Gralla EB, Valentine JS (1996) Mutations in copper-zinc superoxide dismutase that cause amyotrophic lateral sclerosis alter the zinc binding site and the redox behavior of the protein. *Proc Natl Acad Sci USA* 93:12240–12244
- Matsuo H, Tsukada S, Nakata T, Chairoungdua A, Kim DK, Cha SH, Inatomi J, Yorifuji H, Fukuda J, Endou H, Kanai Y (2000) Expression of a system L neutral amino acid transporter at the blood-brain barrier. *Neuroreport* 11:3507–3511
- McGeer PL, McGeer EG (2002) Inflammatory processes in amyotrophic lateral sclerosis. *Muscle Nerve* 26:459–470
- Muller AJ, DuHadaway JB, Donover PS, Sutanto-Ward E, Prendergast GC (2005) Inhibition of indoleamine 2,3-dioxygenase, an immunoregulatory target of the cancer suppression gene Bin1, potentiates cancer chemotherapy. *Nat Med* 11:312–319
- Munn DH, Zhou M, Attwood JT, Bondarev I, Conway SJ, Marshall B, Brown C, Mellor AL (1998) Prevention of allogeneic fetal rejection by tryptophan catabolism. *Science* 281:1191–1193
- Nagano S, Satoh M, Sumi H, Fujimura H, Tohyama C, Yanagihara T, Sakoda S (2001) Reduction of metallothioneins promotes the disease expression of familial amyotrophic lateral sclerosis mice in a dose-dependent manner. *Eur J Neurosci* 13:1363–1370
- Owe-Young R, Webster NL, Mukhtar M, Pomerantz RJ, Smythe G, Walker D, Armati PJ, Crowe SM, Brew BJ (2008) Kynurenine pathway metabolism in human blood-brain barrier cells: implications for immune tolerance and neurotoxicity. *J Neurochem* 105:1346–1357
- Pardridge WM, Fierer G (1990) Transport of tryptophan into brain from the circulating, albumin-bound pool in rats and in rabbits. *J Neurochem* 54:971–976
- Perkins MN, Stone TW (1982) An iontophoretic investigation of the actions of convulsant kynurenines and their interaction with the endogenous excitant quinolinic acid. *Brain Res* 247:184–187
- Rosen DR, Siddique T, Patterson D, Figlewicz DA, Sapp P, Hentati A, Donaldson D, Goto J, O'Regan JP, Deng HX et al (1993) Mutations in Cu/Zn superoxide dismutase gene are associated with familial amyotrophic lateral sclerosis. *Nature* 362:59–62
- Rothstein JD (2009) Current hypotheses for the underlying biology of amyotrophic lateral sclerosis. *Ann Neurol* 65:S3–S9
- Salter M, Pogson CI (1985) The role of tryptophan 2,3-dioxygenase in the hormonal control of tryptophan metabolism in isolated rat liver cells. Effects of glucocorticoids and experimental diabetes. *Biochem J* 229:499–504
- Santamaria A, Galvan-Arzate S, Lisy V, Ali SF, Duhart HM, Osorio-Rico L, Rios C, St'astny F (2001) Quinolinic acid induces oxidative stress in rat brain synaptosomes. *Neuroreport* 12:871–874
- Schrocksadel K, Wirleitner B, Winkler C, Fuchs D (2006) Monitoring tryptophan metabolism in chronic immune activation. *Clin Chim Acta* 364:82–90
- Shaw PJ (2005) Molecular and cellular pathways of neurodegeneration in motor neurone disease. *J Neurol Neurosurg Psychiatry* 76:1046–1057
- Smith AP, Lee NM (2007) Role of zinc in ALS. *Amyotroph Lateral Scler* 8:131–143
- Smythe GA, Braga O, Brew BJ, Grant RS, Guillemin GJ, Kerr SJ, Walker WD (2002) Concurrent quantification of quinolinic, picolinic, and nicotinic acids using electron-capture negative-ion gas chromatography-mass spectrometry. *Anal Biochem* 301:21–26
- Stone TW, Perkins MN (1981) Quinolinic acid: a potent endogenous excitant at amino acid receptors in CNS. *Eur J Pharmacol* 72:411–412
- Streit WJ (2002) Microglia as neuroprotective, immunocompetent cells of the CNS. *Glia* 40:133–139
- Sullivan SM, Lee A, Bjorkman ST, Miller SM, Sullivan RK, Poronnik P, Colditz PB, Pow DV (2007) Cytoskeletal anchoring of GLAST determines susceptibility to brain damage: an identified role for GFAP. *J Biol Chem* 282:29414–29423
- Takikawa O, Yoshida R, Kido R, Hayaishi O (1986) Tryptophan degradation in mice initiated by indoleamine 2,3-dioxygenase. *J Biol Chem* 261:3648–3653
- Watanabe M, Dykes-Hoberg M, Culotta VC, Price DL, Wong PC, Rothstein JD (2001) Histological evidence of protein aggregation in mutant SOD1 transgenic mice and in amyotrophic lateral sclerosis neural tissues. *Neurobiol Dis* 8:933–941
- Widner B, Leblhuber F, Walli J, Tilz GP, Demel U, Fuchs D (2000) Tryptophan degradation and immune activation in Alzheimer's disease. *J Neural Transm* 107:343–353
- Widner B, Leblhuber F, Fuchs D (2002) Increased neopterin production and tryptophan degradation in advanced Parkinson's disease. *J Neural Transm* 109:181–189
- Yoshida R, Hayaishi O (1978) Induction of pulmonary indoleamine 2,3-dioxygenase by intraperitoneal injection of bacterial lipopolysaccharide. *Proc Natl Acad Sci USA* 75:3998–4000
- Zhang D (2007) Early activation of an interferon signaling pathway in a mouse model of amyotrophic lateral sclerosis. *J Neurovirol* 13:48 (abstract S.85)
- Zhang H, Andrekopoulos C, Joseph J, Chandran K, Karoui H, Crow JP, Kalyanaraman B (2003) Bicarbonate-dependent peroxidase activity of human Cu, Zn-superoxide dismutase induces covalent aggregation of protein: intermediacy of tryptophan-derived oxidation products. *J Biol Chem* 278:24078–24089